JOURNAL OF VIROLOGY, Nov. 2004, p. 11583–11590 Vol. 78, No. 21
0022-538X/04/$08.00+0 DOI: 10.1128/JVI.78.21.11583–11590.2004

Infection of Vero Cells by BK Virus Is Dependent on Caveolae

Sylvia Eash,[1,2] William Querbes,[1,2] and Walter J. Atwood[2]*

Graduate Program in Pathobiology[1] and Department of Molecular Microbiology and Immunology,[2] Brown University, Providence, Rhode Island

Received 4 May 2004/Accepted 9 July 2004

Polyomavirus-associated nephropathy occurs in ~5% of renal transplant recipients and results in loss of graft function in 50 to 70% of these patients. The disease is caused by reactivation of the common human polyomavirus BK (BKV) in the transplanted kidney. The early events in productive BKV infection are unknown. In this report, we focus on elucidating the mechanisms of BKV internalization in its target cell. Our data reveal that BKV entry into permissive Vero cells is slow, is independent of clathrin-coated-pit assembly, is dependent on an intact caveolin-1 scaffolding domain, is sensitive to tyrosine kinase inhibition, and requires cholesterol. BKV colocalizes with the caveola-mediated endocytic marker cholera toxin subunit B but not with the clathrin-dependent endocytic marker transferrin. In addition, BKV infectious entry is sensitive to elevation in intracellular pH. These findings indicate that BKV entry into Vero cells occurs by caveola-mediated endocytosis involving a pH-dependent step.

Humans are the natural host species for two members of the polyomavirus family, BK virus (BKV) and JC virus (JCV) (22). Both viruses establish persistent subclinical infections in the kidneys and peripheral blood in 85% of the population worldwide (10, 36). The urotheliotropic nature of BKV is characterized by infection of the epithelial lining of the collective ducts, the transitional epithelial cells of the renal calyces, the parietal epithelium of the Bowman's capsule, and the transitional epithelium of the renal pelvis and the urinary tract (11, 56). Sporadic reactivation of BKV resulting in limited viral replication is seen in 0.5 to 20% of healthy seropositive individuals, yet renal function is left unaffected (20, 23, 62). A dramatic increase in viral activity leading to disease progression occurs predominantly in the context of greatly impaired T-cell-mediated immunity (26, 27).

Kidney transplant recipients are subjected to a potent immunosuppressive therapy and are thus at a high risk for exacerbated BKV replication (1). Active BKV infection in the renal allograft, known as polyomavirus nephropathy, has been linked to progressive graft dysfunction and ultimate graft loss (13). Sustained high levels of viral replication result in lytic destruction of the host tubular cells and release of BKV progeny to perpetuate the infection (1, 33, 34). BKV, the causative agent of polyomavirus nephropathy, is drawing increasing attention as a significant factor in the failure of renal transplants (48).

Similar to those of the other polyomaviruses, BK virions are small (40.5 to 45 nm in diameter) and consist of a superhelical circular double-stranded DNA genome contained within a nonenveloped icosahedral capsid (18). Though the exact identity of the BK receptor(s) is unknown, evidence suggests that gangliosides type II, GD1a, and GT play important roles in the initial interaction between BKV and the permissive monkey kidney (Vero) cell line, as well as in BKV hemagglutination of human type O red blood cells (54, 59, 60). Following penetration of the target cell membrane and BKV internalization, the viral genome is delivered to the host cell nucleus. There, viral transcription, replication, and assembly take place (55). The exact mechanism through which BKV enters a permissive cell remains unknown. There are two ultrastructural accounts of BK virions localized in membrane-bound cytoplasmic structures reminiscent of caveolae (42). However, there is no comprehensive, conclusive study characterizing the mechanism of BKV endocytosis into permissive cells. Extensive work has been dedicated to elucidating the modes of infectious entry of several other closely related members of the polyomavirus family: simian virus 40 (SV40), mouse polyomavirus (Py), and JCV (2, 15, 16, 40, 41, 43, 44, 47, 51). Despite the high similarity among these viruses (21), they employ different endocytic routes to internalize into target cells. Productive infection by SV40 is facilitated by caveola-mediated endocytosis (2, 40, 41, 51), while JCV uptake occurs through the clathrin-dependent route (43, 44). To invade the host, Py utilizes either caveolar endocytosis (47) or an alternative clathrin-, caveolin-1-, dynamin I-independent pathway (15) as dictated by the target cell type.

In this report, we examine the kinetics and mechanism of BKV infectious entry into Vero cells. By using established techniques for studying virus internalization, we found that BKV enters these cells at a relatively slow rate so that the majority of virus successfully escapes the action of neutralizing sera between 2 and 4 h after entry. Pharmacological depletion of membrane cholesterol, a major component of lipid rafts and caveolae (7, 61), completely inhibited infection. We then analyzed the role of clathrin-dependent or caveola-dependent endocytosis in BKV internalization by expressing mutant forms of specific key proteins and thus selectively perturbing each pathway. BKV readily infected cells that were defective in assembling clathrin-coated pits. In contrast, a reduction in infectivity was observed in cells expressing a mutant construct of caveolin-1. The tyrosine kinase inhibitor genistein inhibited infection at the initial stage of the virus life cycle, suggesting that BKV induces intracellular signaling that is important for productive infection. Additional observations revealed an overlap in cellular localization of BKV with the marker for caveola-mediated endocytosis, cholera toxin subunit B (CT-B). Taken

* Corresponding author. Mailing address: Department of Molecular Microbiology and Immunology, Brown University, Box G-B616, 171 Meeting St., Providence, RI 02912. Phone: (401) 863-3116. Fax: (401) 863-1971. E-mail: Walter_Atwood@Brown.edu.

together, these data strongly suggest that during productive infection BKV enters Vero cells through a caveola-mediated pathway of endocytosis.

MATERIALS AND METHODS

Cells, viruses, and antibodies. Vero cells were obtained from the American Type Culture Collection (Manassas, Va.) and were maintained in a humidified 37°C CO_2 incubator in Eagle's minimal essential medium (EMEM) (Mediatech Inc., Herndon, Va.) supplemented with 5% heat-inactivated fetal bovine serum (Mediatech Inc.). BKV Gardner strain was purchased from the American Type Culture Collection and propagated in Vero cells as described previously (45). The monoclonal antibody PAb 416 purchased from Oncogene Research Products (Cambridge, Mass.) detects the N-terminal portion of SV40, JCV, and BKV large T antigen (T-Ag). The BKV major capsid protein VP1 is recognized by the monoclonal anti-JCV/BKV antibody from Novocastra Laboratories Ltd. (Newcastle, United Kingdom). Rabbit anti-BKV serum was produced by injecting a New Zealand White rabbit with a highly purified preparation of BKV in complete Freund's adjuvant (17). The rabbit received two additional BKV boosts in incomplete Freund's adjuvant. The titer of the anti-BKV serum was determined by a Western blot assay, and the immunoglobulin G portion was purified and isolated on a protein G column (Pierce Biotechnology, Rockford, Ill.).

Virus purification and labeling. Vero cells were plated and infected with 8,192 hemagglutination units (HAU) of BKV, corresponding to a multiplicity of infection (MOI) of 200, for 1 h at 37°C. Four weeks later, the cells were harvested by scraping as they began to exhibit extensive cytopathic effect and were concentrated by centrifugation at 960 × *g* for 30 min. Following resuspension in 20.0 ml of the supernatant, the pellet comprised of virus-infected cells underwent three freeze-thaw cycles. To ensure further lysis and release of viral particles, the cells were subjected to brief sonication. Deoxycholic acid was added to the lysate at a final concentration of 0.25%, and the mixture was incubated for 30 min at 37°C. The viral particles were isolated from the cellular debris by centrifugation at 1,960 × *g*. The supernatant containing BK virions was layered over 20% sucrose and pelleted for 3 h at 70,000 × *g*. Following resuspension in buffer A (1 M Tris, pH 8, 5 M NaCl, 0.1 M $CaCl_2$) supplemented with 0.01% Triton X-100, the viral stock was distributed over a CsCl density gradient (1.35, 1.32, 1.29, 1.26, and 1.23 mg/ml). The virions were allowed to reach their buoyant density of 1.34 mg/ml of CsCl by centrifugation at 120,000 × *g* for 15 h. The virus band was extracted and dialyzed overnight against buffer A. The protein concentration of the purified virus stock was determined by the Bradford assay. Fluorochrome conjugation of BKV with Alexa Fluor 488 carboxylic acid-succinimidyl ester was performed according to the manufacturer's labeling procedure (MP00143; Molecular Probes, Eugene, Oreg.). Briefly, 5.0 mg of gradient-purified BKV was dialyzed against labeling buffer (0.1 M $NaHCO_3$, pH 8.3) at 4°C overnight. The virus was then incubated for 1 h on a platform rocker at room temperature with 1 μg of Alexa Fluor 488 (AF488) succinimidyl ester (Molecular Probes) in 100 μl of dimethyl sulfoxide. The AF488-labeled virus was extensively dialyzed against two changes of buffer A. The degree of virus labeling was determined as the number of dye molecules per protein molecule and was found to be satisfactory.

Time course of BKV infectious entry into Vero cells. Vero cells that had been seeded on coverslips the previous day were prechilled for 15 min at 4°C and incubated with 123 HAU of cold BKV, corresponding to an MOI of 4, for 45 min at 4°C. The cells were then warmed up to 37°C and incubated in the presence of growth medium. The virus inoculum was removed by washing, and neutralizing anti-BKV serum (1:10, 000) was added to the cells at 0, 0.5, 1, 2, and 4 h post-37°C shift. Two days later, the cells were fixed in 2% paraformaldehyde (PFA), and the number of infected cells was determined by staining for T-Ag expression.

Internalization of CT-B and transferrin and colocalizaion with AF488-BKV. Vero cells were plated on coverslips the day before being used. In the case of AF488-BKV colocalization with endocytic markers, the cells were prechilled and incubated with AF488-BKV in combination with 5.0 μg of Alexa Fluor 594-conjugated cholera toxin subunit B (AF594–CT-B; Molecular Probes)/ml or 7.0 μg of Alexa Fluor 594-conjugated transferrin (AF594-Tf; Molecular Probes)/ml for 30 min in the cold to synchronize entry. The cells were then shifted to 37°C for 4 or 6 h. Unbound virus and endocytic markers were washed off, and the cells were fixed in 2% PFA-PBS and analyzed at a magnification of ×63 on a laser scanning confocal microscope (LSCM), (TCS SP2 AOBS; Leica Microsystems, Exton, Pa.). The images were processed with Adobe Photoshop version 6.0. Internalization of AF594–CT-B and AF594-Tf into Cav-1- or Eps15-transfected or methyl-beta-cyclodextrin (MβCD)-treated Vero cells was performed according to the same protocol with the exception of the entry synchronization step, and the incubation times varied as noted for each figure.

Neutralization of intracellular pH. Vero cells were treated with 25 mM NH_4Cl (Sigma) or 100 μM chloroquine (Sigma-Aldrich) for 3 h at 37°C. To confirm an elevation in intracellular pH, the cells were incubated with 100 nM LysoSensor Green DND-189 (Molecular Probes) for 30 min at 37°C in the continuous presence of the drugs. The internalization pattern of the pH indicator was analyzed in live cells with an inverted fluorescence microscope (Eclipse TE20000-U; Nikon, Melville, N.Y.). Following the 3-h pretreatment, the Vero cells were challenged with 123 HAU of BKV for 4 h in the continuous presence of the drugs. The virus inoculum and drugs were removed by washing, and infection was allowed to proceed for 48 h in medium containing anti-BKV neutralizing serum. The cells were then fixed and stained for the expression of the early viral protein BKV T-Ag.

Pharmacological treatment of Vero cells during BKV infection. Vero cells that had been seeded on coverslips the previous day were exposed for 45 min to MβCD (5 mM in water) or for 1 h to genistein (100 or 200 μM in dimethyl sulfoxide) at 37°C. The cells were then challenged with 123 HAU of BKV for 4 h in the continuous presence of the drugs. At the end of the 4 h, the cells were washed twice with 5% EMEM and incubated with 5% EMEM containing anti-BKV neutralizing serum for 48 h. The cells were then fixed and stained for expression of early BKV T-Ag.

Indirect immunofluorescence analysis of viral infection. To detect expression of early T-Ag or late V-Ag, BKV-infected Vero cells were fixed in 2% PFA at the end of a 48- or 72-h incubation period, respectively, after BKV infection. In the case of SV40, T-Ag expression was analyzed 24 h postinfection using the same protocol as for BKV. Following three washes in phosphate-buffered saline (PBS) (137 mM NaCl, 2.682 mM KCl, 8.1 mM Na_2HPO_4, 1.47 mM KH_2PO_4, pH 7.2), the cells were incubated with a 1:20 dilution of PAb 416 or a 1:15 dilution of anti-JCV/BKV for 1 h at 37°C. The cells were then washed three times in PBS, followed by a 45-min incubation at 37°C with a 1:150 solution of goat anti-mouse immunoglobulin G $F(ab')_2$ fragments conjugated to Alexa Fluor 488 or Alexa Fluor 594 (Molecular Probes). After that, the cells were extensively rinsed in PBS and counterstained with Evan's Blue solution (red cytoplasmic dye). The coverslips were mounted on glass slides with glycerol-PBS (9:1). Cells expressing T-Ag or V-Ag were visualized with a Nikon epifluorescence microscope (Eclipse E800; Nikon, Inc.). A minimum of eight fields were counted for each sample from three or more independent experiments.

Transfection of Eps15 and caveolin-1 plasmid constructs. The GFP-Eps15 constructs D3Δ2, DIII, and EΔ95/295 were a generous gift from A. Benmerah (5, 6). Briefly, Eps15 is composed of three structural domains designated DI, DII, and DIII in N- to C-terminal sequence (6). We obtained two dominant-negative mutant constructs: EΔ95/295, an Eps15 deletion mutant lacking the second and third EH domains, which constitute the protein-protein interaction module of the intact protein, and DIII, a truncated form of Eps15 which spans the carboxyl-terminal domain responsible for interaction with the plasma membrane adaptor complex, AP2. The DIIIΔ2 control deletion construct lacks DI, DII, and the AP-2 binding portion of DIII and therefore does not interfere with clathrin-dependent endocytosis (6, 8). The wild-type and F92A-V94A Myc-tagged caveolin-1 constructs were generous gifts from M. J. Quon (35). For all plasmid transfections, Vero cells were seeded on glass coverslips at 5×10^5/per well of a six-well dish the day before the procedure. For all wells, equal amounts of DNA (1.6 μg) were precomplexed with Plus reagent and then combined with Lipofectamine reagent (Invitrogen, Carlsbad, Calif.) according to the manufacturer's instructions. The DNA complexes were added to the cells in serum-free EMEM for 6 h at 37°C. After the incubation period, the transfection complex was washed off and the cells were refed with fresh 5% EMEM. At 24 h posttransfection, the cells were infected with BKV, or SV40 in the case of the Cav-1-transfected cells. One (SV40) or 2 (BKV) days later, the cells were fixed and stained for T-Ag as described above. Green fluorescent protein (GFP) activity was indicative of Eps15 construct expression. As for the Cav-1 constructs, expression was detected with a 1:50 dilution of rabbit anti-Myc antibody (Sigma-Aldrich) for 1 h at 37°C, followed by a 45-min incubation with a 1:150 dilution of goat anti-rabbit AF-488 secondary antibody (Molecular Probes).

RESULTS

Time course of BKV entry into Vero cells. Our initial step in characterizing the mechanism of BKV entry was to determine the kinetics of viral internalization into the permissive monkey kidney Vero cell line. Vero cells were prechilled, and 123 HAU of BKV (MOI, 4) was added to the cells and allowed to adsorb without internalization for 1 h at 4°C. Infection was then ini-

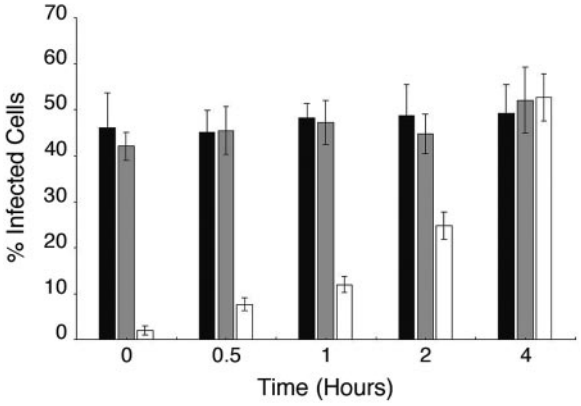

FIG. 1. Time course of BKV infectious entry into Vero cells. Prechilled Vero cells were inoculated with BKV for 1 h at 4°C. The cells were then warmed to 37°C, and regular medium (dark bars) or medium containing preimmune serum (grey bars) or anti-BKV serum (open bars) was added at the indicated time points and left on for the duration of the infection. The percentage of infected cells was scored at 48 h postinfection by indirect immunofluorescent staining of T-Ag-expressing cells. The value of each bar in the graph represents the percentage of infected cells per field and was calculated as the average of at least eight nonoverlapping random fields of cells from each of three independent experiments. The error bars represent the standard deviation.

tiated by incubating the cells at 37°C. Neutralizing anti-BKV serum was added to the cells at various time increments: 0, 0.5, 1, 2, and 4 h following the 37°C shift. Control cells were treated with medium containing either no anti-BKV serum or preimmune rabbit serum. Infection was scored 48 h later by staining the cells for the expression of BKV early T-Ag. When added immediately prior to the 37°C shift, the anti-BKV serum nearly completely blocked BKV infection of Vero cells (Fig. 1). The presence of preimmune rabbit serum in the medium did not interfere with the efficiency of BKV infection (Fig. 1). Our results reveal that the majority of the virus is internalized in the cells between 2 and 4 h after the initiation of infection, as measured by the ability of the virus to escape antibody-mediated neutralization (Fig. 1).

BKV infection of cholesterol-depleted Vero cells. Caveolae are described as cholesterol- and sphingolipid-rich smooth invaginations of the plasma membrane that are formed upon polymerization of caveolins (29, 63). Depletion of plasma membrane cholesterol by MβCD physically disrupts caveolae and therefore interferes with caveola-mediated endocytosis. (MβCD is a cyclic oligosaccharide that has seven hydrophobic-molecule binding pockets.) To establish a role for cholesterol in BKV infection, Vero cells were pretreated with 5 mM MβCD for 30 min at 37°C. Cholesterol depletion resulting in perturbed caveola-mediated endocytosis was confirmed by a significant reduction in uptake of AF594-labeled CT-B by treated cells (Fig. 2, top). Following MβCD treatment, the Vero cells were infected with BKV for 4 h at 37°C in the continuous presence of the drug. The cells were then washed and incubated with medium containing BKV-neutralizing serum for an additional 48 h. Control cells were mock treated and infected with the virus. Infection was scored by staining for expression of the early BKV T-Ag. BKV infection was inhibited in cells treated with MβCD (Fig. 2, bottom).

BKV infection of Vero cells expressing dominant-negative Eps15 constructs. The most common pathway used by both enveloped and nonenveloped viruses to enter a cell is clathrin-mediated endocytosis (28). Dominant-negative mutants of Eps15 inhibit transferrin uptake and block the entry of viruses that internalize via clathrin-dependent endocytosis (6, 8). The eps15 mutant constructs do not interfere with the entry of viruses that utilize clathrin-independent endocytosis, such as SV40 and influenza virus (41, 57). We used one control (DIIIΔ2) and two dominant-negative (DIII and EHΔ95/295) GFP-Eps15 fusion constructs to transiently transfect Vero cells (Fig. 3, top). To ensure disruption of the clathrin-dependent endocytic pathway, we allowed 24 h for maximal plasmid expression and then incubated the cells with AF594-transferrin. As expected, the DIII and EHΔ95/295 constructs, but not the DIIIΔ2 Eps15 mutants, successfully inhibited transferrin uptake (Fig. 3, middle). At 24 h posttransfection, Vero cells expressing the Eps15 constructs were infected with BKV. Infection was scored 72 h later by indirect immunofluorescence analysis for V-Ag expression. The results from our single-cell infectivity assay revealed that cells double positive for dominant-negative-Eps15 and V-Ag expression were readily detectable in the presence of the control, as well as the two mutant constructs (Fig. 3, bottom). These findings indicate that BKV infection proceeds successfully in the absence of clathrin-coated pit assembly.

BKV infection of Vero cells expressing recombinant caveolin-1 constructs. Caveolin-1 (Cav-1), a 21- to 24-kDa protein, is the defining structural component of caveolae and is directly involved in their biogenesis (46, 49). The scaffolding domain (residues 82 to 101) of Cav-1 recognizes and binds to specific caveolin-binding motifs present in the catalytic domains of several signaling molecules, such as G proteins, Src-like kinases, receptor tyrosine kinases, and actin-binding proteins

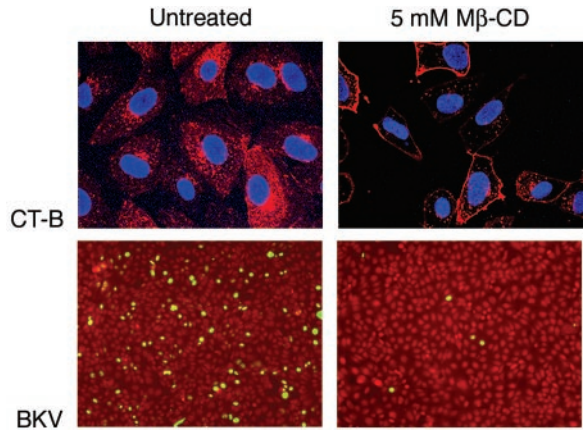

FIG. 2. MβCD inhibits BKV infection. Vero cells grown on coverslips were mock treated or treated with 5 mM MβCD for 30 min at 37°C. The cells were then incubated with AF594–CT-B (top) for 1 h at 37°C in the continuous presence of the drug. The cells were washed and fixed in 2% PFA. CT-B internalization was observed using an LSCM with a 63× objective. Alternatively, following pretreatment, the cells were incubated with BKV (bottom) for 4 h in the absence or presence of the drug. The treatment medium and viral inoculum were removed by washing. The cells were refed with fresh medium containing anti-BKV serum to neutralize the remaining extracellular virus, and infection was allowed to proceed for an additional 48 h. Infected cells were visualized by staining for expression of the early viral protein T-Ag.

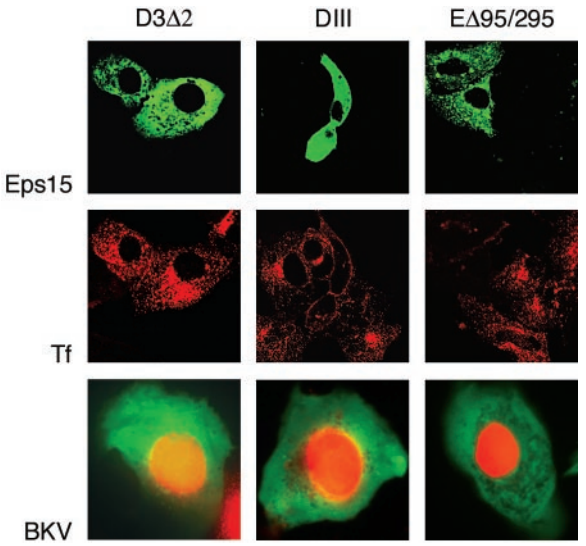

FIG. 3. BKV infects Vero cells expressing Eps15 constructs. Vero cells seeded on coverslips were transfected with GFP-tagged control (D3Δ2) or dominant-negative (DIII and EΔ95/295) Eps15 constructs (top). After 24 h, the cells were incubated with AF594-Tf (middle) for 45 min at 37°C, washed, and fixed, and the Tf internalization pattern was observed by confocal microscopy. Transfected cells were also infected with BKV (bottom). Infection was scored 72 h later by staining with an anti-V-Ag monoclonal antibody (red) that detects the late viral capsid protein VP1. The GFP-expressing cells were directly visualized under an epifluorescence microscope. Green, cells positive for expression of Eps15 constructs; red, cells positive for V-Ag expression.

(25, 38, 53). We transiently transfected Vero cells with mammalian expression vectors containing cDNA for Myc-tagged wild-type canine Cav-1 (wt Cav-1) or for mutant Cav-1 (mut Cav-1). The two point mutations F92A and V94A in the scaffolding domain of mut Cav-1 disrupt the binding of Cav-1 to caveolin-1 binding motifs (35). Plasmid expression was allowed to proceed for 24 h, after which the cells were either incubated with the endocytic marker AF594–CT-B or AF594-Tf for 1 h or infected with BKV for 48 or SV40 for 24 h. The cells were then fixed and stained with anti-Myc tag antibody alone (Fig. 4A, rows 2 and 4) or double stained with anti-BKV or -SV40 T-Ag and anti-Myc tag antibodies (Fig. 4B, bottom). Expression of the mutant Cav-1 construct successfully blocked AF594–CT-B internalization (Fig. 4A, row 3); AF594-Tf uptake was unaltered (Fig. 4A, row 1). Both endocytic markers entered mock- and wt Cav-1-transfected cells (Fig. 4A, rows 1 and 3). In the case of infection, double-positive cells were counted using an indirect immunofluorescence assay. There were 85 and 84% reductions in the numbers of mut Cav-1-transfected cells expressing BKV or SV40 T-Ag, respectively, compared to those transfected with wt Cav-1. These results suggest that an intact caveolin-1 scaffolding domain is important for proper BKV infection.

BKV infection in the presence of a tyrosine kinase inhibitor. The related polyomaviruses JCV and SV40 have been shown to induce signaling that is important for viral entry. Since our caveolin-1mutant construct inhibits the interaction of caveolin-1 with several key early signaling molecules (i.e., protein kinase C and Src family kinases), we sought to examine whether BKV also induced a signal that was important for its entry. Previously, the tyrosine kinase inhibitor genistein was shown to block signals induced by JCV and SV40; we asked whether the drug would also block BKV entry. This experiment was done using an infectious-entry assay, in which virus was allowed to enter in the presence or absence of the drug for 4 h and then membrane-bound or extracellular virus was neutralized with antiserum against either SV40 or JCV. Infection was scored using an indirect immunofluorescence assay for the early viral protein T-Ag. As can be seen in Fig. 5, infectious entry of BKV was inhibited in the presence of genistein, indicating that BKV-induced transmembrane signaling is important for efficient virus entry into host cells.

Colocalization of BKV with endocytic markers. The internalization pathways utilized by *Vibrio cholerae* toxin and Tf have been well characterized (31, 32, 37, 50). The *V. cholerae* toxin homopentameric B subunit specifically binds to glycolipid monoganglioside at the plasma membrane and is internalized and then delivered to the Golgi complex through caveola-mediated endocytosis (31, 32). Transferrin is a known marker for clathrin-dependent receptor-mediated endocytosis (50). We labeled CsCl-purified BK virions with Alexa Fluor 488 fluorochromes. Vero cells were incubated with AF488-BKV and with either AF594–CT-B or AF594-Tf for 30 min at 4°C to ensure binding without endocytosis. Synchronized entry was initiated by warming the cells to 37°C and was allowed to proceed for 4 or 6 h. Each endocytic marker, CT-B or Tf, was present in the medium for the entire course of virus internalization. The cells were then washed, fixed, and analyzed by laser scanning confocal microscopy. Colocalization was seen between the marker for caveola-mediated endocytosis (CT-B) and BKV (Fig. 6B). The clathrin-dependent endocytosis marker, Tf, did not appear to overlap with BKV inside the cell (Fig. 6A).

BKV infection in the presence of lysosomotropic agents. Ultrastructural analysis of BKV-infected tissue specimens revealed viral particles within cytoplasmic-membrane-bound organelles, implying a receptor-mediated entry pathway (42). Not only would cellular transport vesicles allow the virus to systematically advance through the cytosol, their acidic environment might also facilitate virus uncoating (39). We assessed the role of low pH in BKV infectious entry by using lysosomotropic agents to disrupt the acidification of intracellular organelles. Chloroquine (CQ) and ammonium chloride (NH_4Cl) are weakly basic amines that, in their neutral forms, selectively enter cellular compartments with low internal pH and there become protonated, thereby elevating the pH of the target organelle. Vero cells were incubated for 3 h at 37°C in the presence of 100 μM CQ, 25 mM NH_4Cl, or control medium. Neutralization of the pH in acidic organelles was confirmed by a fluorescent pH indicator probe, LysoSensor (Fig. 7, top). Pretreated cells were infected with BKV in the presence of CQ or NH_4Cl. Untreated cells were infected with BKV in the absence of any drugs. Infection was scored 48 h later by staining for BK T-Ag expression. Treatment with either lysosomotropic agent inhibited BKV infection by 80% compared to untreated controls (Fig. 7, middle, and graph). In a parallel control experiment, this same treatment had no effect on infection of Vero cells by SV40 (not shown). The results of this experiment indicate that infectious entry of BKV into Vero cells is sensitive to elevation of pH.

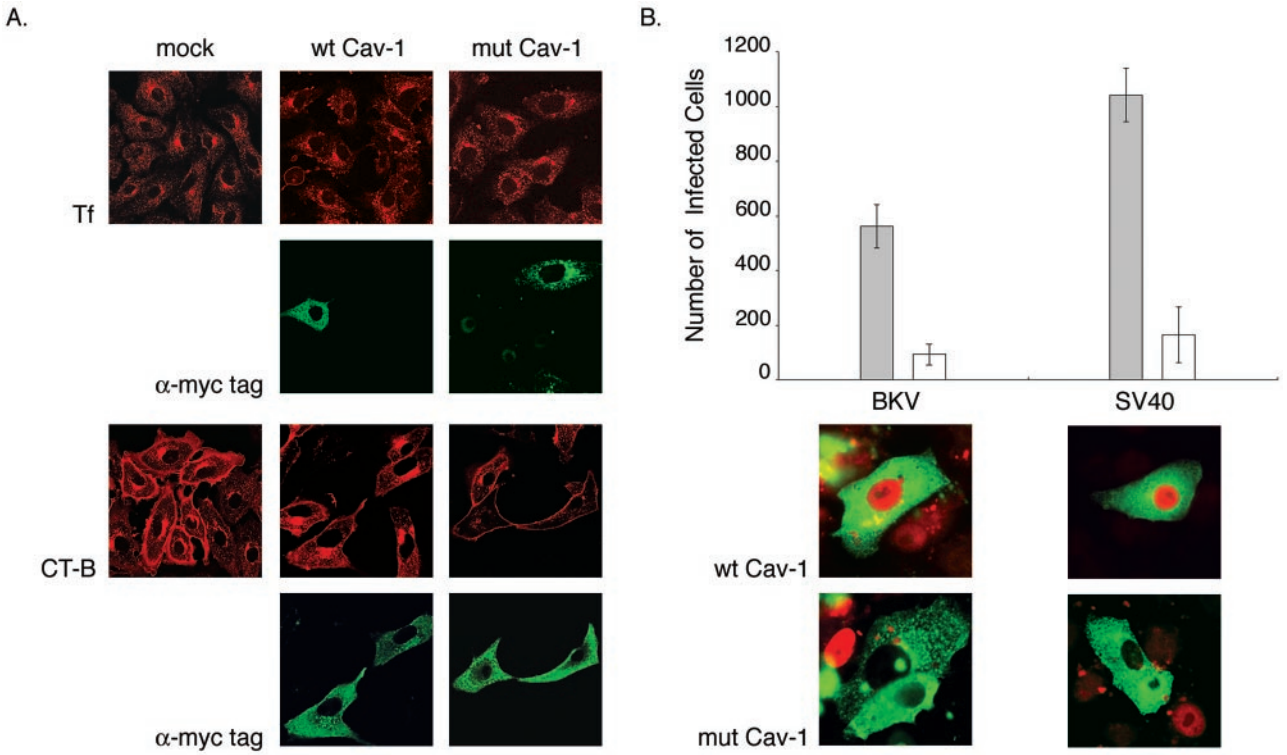

FIG. 4. BKV infection is reduced in Vero cells expressing F92A-V94A caveolin-1 construct. (A) Vero cells were transiently transfected with equal amounts of either wild-type or mutant caveolin-1 plasmid DNA. Twenty-four hours later, construct expression was detected by staining the cells with anti-Myc tag antibody (rows 2 and 4). Cells were incubated with AF594-Tf (row 1) or AF594–CT-B (row 3) for 1 h at 37°C as controls and then fixed in 2% PFA. The internalization patterns of the endocytic markers were visualized using a confocal microscope. (B) Alternatively, transfected cells were infected with BKV or SV40; fixed 48 or 24 h later, respectively; and stained for both Myc tag and T-Ag expression (bottom). Each bar of the graph represents the mean number of double-positive cells contained on a 22-mm^2 glass coverslip in each of three independent experiments. The error bars refer to the standard deviation. Shaded bars, Vero cells expressing wt Cav-1; open bars, Vero cells expressing mut Cav-1.

DISCUSSION

Successful virus receptor interaction is the prelude to a series of consecutive purposeful steps resulting in virus multiplication, collectively described as the viral life cycle. The proper execution of each stage of the infectious cycle depends on the virus exploitation and manipulation of the host cell machinery. To replicate and propagate, BKV must enter the target cell and reach its nucleus. The set of experiments described in this report expands our knowledge of BKV biology by characterizing the mechanism of BKV internalization into the permissive host during productive infection. Our findings argue in favor of caveola-mediated endocytosis for BKV uptake into Vero cells.

This internalization pathway is defined by its cholesterol sensitivity, clathrin independence, and caveolin-1 and dynamin dependence (29). In addition, ligand internalization through caveolae, although very efficient, is a slower process than other equally well-characterized uptake mechanisms (14, 64).

First, we examined the kinetics of BKV infectious entry into Vero cells. Our results show that BKV is unlike the rapidly internalizing JCV but is similar to SV40, which enters the cells at a lower rate (43). The majority of BK infection-competent virions reached an antibody neutralization-resistant compartment between 2 and 4 h after the initiation of synchronized infection. Delayed internalization kinetics has been ascribed to SV40, which enters the cell via caveola-mediated endocytosis (2, 43). In contrast, the clathrin-dependent uptake of JCV allows the virus to escape the action of the neutralizing sera as early as 30 min after the start of active endocytosis (43).

Next, we evaluated the need for intact cell surface cholesterol composition during the early steps of BKV infection. The inhibitory effect of the cholesterol-depleting agent MβCD on BKV infection suggested the involvement of cholesterol-rich membrane subdomains, such as lipid rafts and/or caveolae, in virus internalization. Infection of susceptible cells by SV40 is also highly sensitive to disruption of caveolar function resulting from alterations in the cholesterol content of the target membrane (16). In the case of Py, both cholesterol-dependent and -independent entry pathways have been described depending on the target cells (16, 47). As expected, cholesterol is indispensable for successful internalization through the caveolar mechanism (47), while Py infection via the clathrin-, caveolin-1-, and dynamin I-independent pathway does not display the same requirement (15, 16).

Ligand internalization through caveolae or lipid rafts may share cholesterol dependence, yet other pathway-defining components determine the subsequent intracellular fate of the cargo (30, 39). To better understand the uptake of BKV into Vero cells, we asked whether clathrin pit assembly was necessary for BKV infection. Dominant-negative constructs of Eps15,

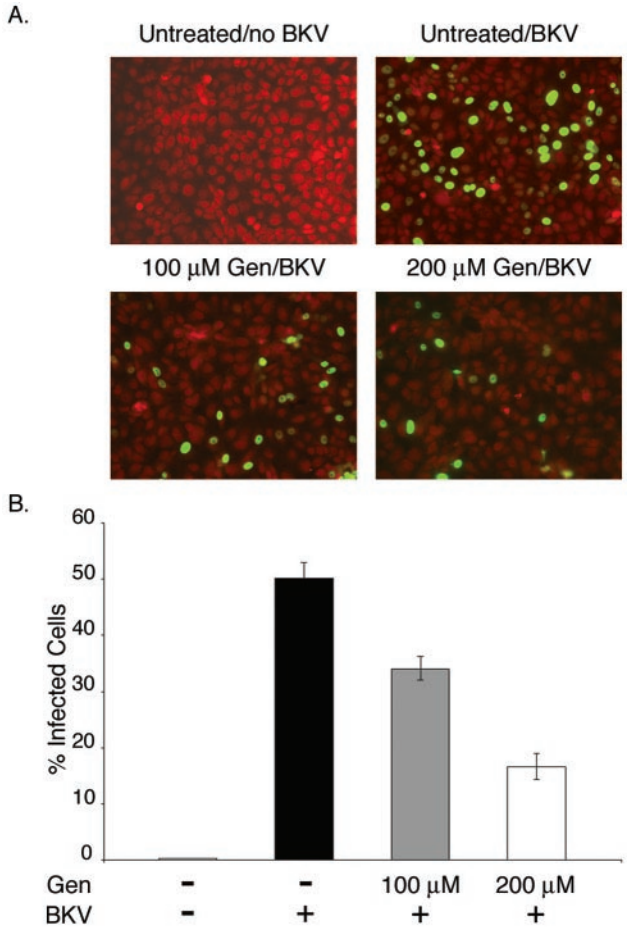

FIG. 5. Genistein inhibits BKV infection of Vero cells. (A) Vero cells seeded on coverslips were mock treated (top row) or pretreated with 100 or 200 μM genistein (bottom row) for 1 h at 37°C. The cells were then incubated with BKV for 4 h at 37°C with or without drug. After removal of the viral inoculum, the cells were refed with fresh medium supplemented with anti-BKV serum. The cells were fixed 48 h later, and infection was scored by indirect immunofluorescent staining for T-Ag. Fields of cells representing each experimental condition are shown. (B) Each bar of the graph indicates the percentage of infected cells per field and represents the mean of at least eight random fields from each of three independent experiments. The error bars refer to the standard deviation value. Gen, genistein; +, present; −, absent.

a protein required for the early steps of clathrin-dependent endocytosis (6), were introduced into Vero cells to disrupt internalization through this mechanism. BKV was able to establish infection in cells expressing the mutant forms of Eps15, suggesting that virus entry occurred independently of the clathrin-dependent route. Similarly, endocytosis and infection by SV40 were found to be insensitive to perturbation of the clathrin-dependent route (41). In contrast, JCV infection was blocked by the transient expression of dominant-negative Eps15 mutants, supporting earlier pharmacological data that proposed clathrin-dependent endocytosis as the uptake mechanism for the virus (43, 44).

We then turned our attention to the role of caveola-mediated endocytosis as a mechanism of BKV internalization into host cells. Infection of CV1 and Vero cells by SV40 was significantly inhibited when preceded by the transfection of a caveolin mutant lacking the scaffolding domain of the protein. In cells transfected with wild-type caveolin, SV40 infection levels remained the same as those of untransfected cells (51). In our investigations, reduced susceptibility to BKV infection was observed in Vero cells transfected with the F92A-V94A caveolin-1 mutant, while cells expressing the wild-type construct remained targets for the virus. The substitution mutations in the scaffolding region of the mut Cav-1 construct were designed to compromise the direct binding of caveolin-1 to the ΦXΦXXXXΦ (Φ is an aromatic amino acid, Trp, Tyr, or Phe, and X is any amino acid) caveolin-1 binding motif present on many caveola-associated proteins, such as G proteins, Src-like kinases, eNOS, protein kinase Cα, MAPK, EGF receptor, and PDGF receptor (4, 53). Binding to the scaffolding domain is considered to provide the mechanism for caveolin-1 not only to nucleate and incorporate relevant signaling molecules within caveolae, but also to regulate their activation upon ligand binding (4). Indeed, SV40 binding to caveolae is followed by a virus-induced signal for tyrosine phosphorylation of proteins sequestered within caveolae (38, 41). Furthermore, only virion-loaded caveolae immunostained positive for phosphotyrosines and subsequently internalized. Caveolae which did not contain SV40 particles remained at the cell membrane (38, 41). Given this model, the inhibition of BKV infection seen in cells ex-

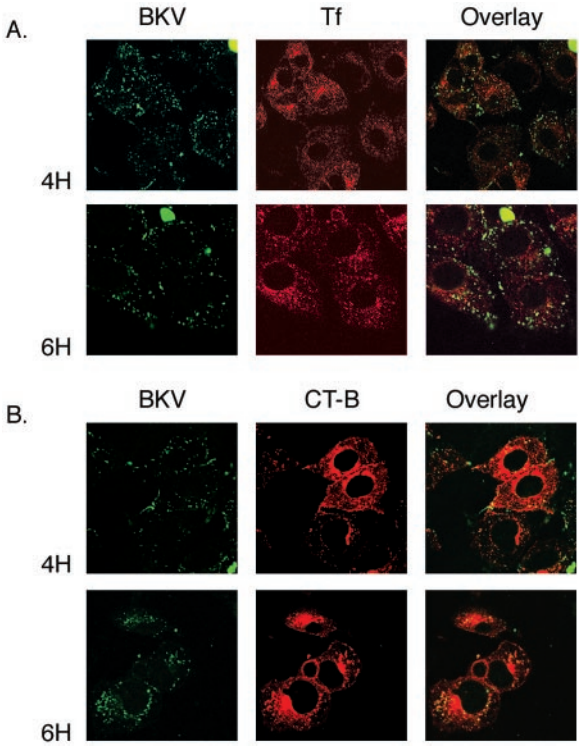

FIG. 6. BKV colocalizes with CT-B, a marker of caveola-mediated endocytosis. Vero cells seeded on coverslips were incubated with AF488-labeled BK in combination with either AF594-labeled CT-B or AF594-labeled Tf for 30 min at 4°C. Synchronized entry was initiated by shifting the cells to 37°C. The cells were washed and fixed in 2% PFA at the indicated time points. Internalization of the markers and the virus was analyzed using an LSCM with a 63× objective. Overlap (yellow) between BKV and CT-B, but not between BKV and Tf, is seen in the merged images.

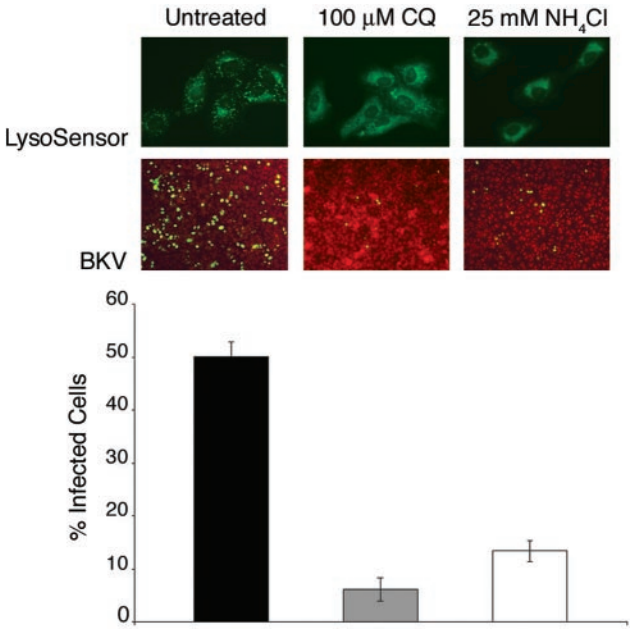

FIG. 7. Neutralization of pH in cellular acidic compartments decreases BKV infection of Vero cells. Vero cells were treated with 100 μM CQ or 25 mM NH_4Cl for 30 min at 37°C. The cells were then incubated with 100 nM LysoSensor solution for 30 min at 37°C in the continuous presence of the drugs. Internalization and activity of the LysoSensor probe was analyzed in live cells using an inverted fluorescence microscope (top). Following pretreatment, Vero cells were infected with BKV for 4 h in the continuous presence of the drugs. The cells were then washed and incubated in medium containing neutralizing BKV serum for the duration of the infection. The cells were fixed 48 h later and stained for T-Ag expression (middle). The results from three independent experiments were calculated and are displayed in the bar graph (bottom). The error bars represent standard deviations of the mean values.

pressing the mut Cav-1 constructs could be attributed to the inability of F92A-F94A caveolin-1 to bind and cluster key receptor and/or signaling molecules required for BKV-triggered internalization of caveolae. In support, exposing the cells to the tyrosine kinase inhibitor genistein during the initial 4 h of infection was sufficient to block productive entry by BKV. These results are suggestive of underlying signaling events necessary for BKV uptake into the host cell. As mentioned earlier both SV40 and JCV induce signaling events required for their own endocytosis (9, 41, 44).

Monitoring the fate of BKV inside the cells revealed overlap between endocytosed CT-B and fluorochrome-labeled virions. No colocalization was observed between internalized transferrin and BKV. Although a few studies have reported partial uptake of CT-B via the classic clathrin pathway in cells with low expression of caveolin-1, such as HeLa and Calu-6 cells, this bacterial toxin is endocytosed through the caveola-mediated route in most of the other cell types analyzed (52, 58). CT-B internalization in Vero cells, rat fibroblasts, human skin fibroblasts, and Cos-7, NIH 3T3, MDCK, and Calu-1 cells was shown to be unaffected by the action of nystatin, genistein, K^+ depletion, hypertonic treatment, or dominant-negative Eps-15, all inhibitors of the clathrin-dependent pathway (24, 52, 58). The observed colocalization between BKV and CT-B inside Vero cells implies similarity, at least in part, between the uptake mechanism and intracellular targeting of the two ligands. In addition, incubation of cells with both SV40 and CT-B revealed colocalization of the two markers within caveolin-1-positive discreet compartments (31). Conversely, analysis of the intracellular fate of Hantaan virus, which enters host cells via the clathrin-dependent mechanism, demonstrated extensive overlap between endocytosed virions and transferrin and clear segregation in the localization of Hantaan virus and that of CT-B (19).

The results from our final experiment demonstrate that infection by BKV is sensitive to elevation of the pH in intracellular acidic compartments. Traditionally, viral entry thorough caveolae is considered to occur in a pH-neutral setting, bypassing the acidic endosomal route (3, 40). Nonetheless, newly recognized nonclassical caveolin-1-positive endosomes have been shown to deliver caveola-internalized cargo to the Golgi complex, an organelle with acidic pH ranging form 6.0 to 6.7 *trans* to *cis* (24, 31). The active retrograde transport from the *cis*-Golgi back to the endoplasmic reticulum, an organelle intimately connected with the nucleus, point to the Golgi complex as a potential site for viral uncoating, an event facilitated by low pH (65). Interestingly, a recent ultrastructural analysis of sample tissues from patients with BKV allograft nephropathy demonstrated aggregates of BK virions contained within an elaborate tubular network that was in close proximity to and/or continuous with the Gogli complex in infected cells (12). Taken together, these findings hint at a possible involvement of the Golgi complex in the cytoplasmic traffic of BKV to the site of viral replication and multiplication, the nucleus of the host cell.

Finally, the data presented here suggest that BKV internalization during productive infection occurs through the caveolar mechanism. Our results are consistent with previous morphological observations implicating caveolae in the cellular uptake of BKV (12, 42). The detailed mechanism through which BKV targets its genome to the nucleus remains to be elucidated. Present and future studies in our laboratory are focused on describing early cytoplasmic transport and signaling events responsible for BKV internalization.

ACKNOWLEDGMENTS

We thank all members of the Atwood laboratory for critical discussions during the course of this work. We thank Michael Quon for the wild-type and dominant-negative caveolin 1 mutants and Alexandre Benmerah and Pier Paulo Di Fiore for the Eps15 dominant-negative constructs. We also thank Robbert Creton for critical help with confocal microscopy and Amanda Robinson, Amy Bozek, and Lorie St. Pierre for administrative assistance.

Work in our laboratory was supported by a grant from the National Cancer Institute, R01 CA71878, and by a grant from the National Institute of Neurological Disorders and Stroke, R01 NS43097. W.Q. is supported by a GAANN training grant from the Department of Education, P200A030100.

REFERENCES

1. **Agha, I. A., and D. C. Brennan.** 2002. BK virus and current immunosuppressive therapy. Graft **5:**S65–S72.
2. **Anderson, H. A., Y. Chen, and L. C. Norkin.** 1996. Bound Simian Virus 40 translocates to caveolin enriched membrane domains, and its entry is inhibited by drugs that selectively disrupt caveolae. Mol. Biol. Cell **7:**1825–1834.
3. **Ashok, A., and W. J. Atwood.** 2003. Contrasting roles of endosomal pH and the cytoskeleton in infection of human glial cells by JC virus and simian virus 40. J. Virol. **77:**1347–1356.
4. **Bender, F., M. Montoya, V. Monardes, L. Leyton, and A. Quest.** 2002. Caveolae and caveolae-like membrane domains in cellular signaling and disease: identification of downstream targets for the tumor suppressor protein caveolin-1. Biol. Res. **35:**139–150.

5. **Benmerah, A., C. Lamaze, B. Begue, S. L. Schmid, A. Dautry-Varsat, and N. Cerf-Bensussan.** 1998. AP-2/Eps15 interaction is required for receptor-mediated endocytosis. J. Cell Biol. **140:**1055–1062.
6. **Benmerah, A., V. Poupon, N. Cerf-Bensussan, and A. Dautry-Varsat.** 2000. Mapping of Eps15 domains involved in its targeting to clathrin-coated pits. J. Biol. Chem. **275:**3288–3295.
7. **Brown, D. A., and E. London.** 1997. Structure of detergent-resistant membrane domains: does phase separation occur in biological membranes? Biochem. Biophys. Res. Commun. **240:**1–7.
8. **Carbone, R., S. Fre, G. Iannolo, F. Belleudi, P. Mancini, P. G. Pelicci, M. R. Torrisi, and P. P. Difiore.** 1997. eps15 and eps15R are essential components of the endocytic pathway. Cancer Res. **57:**5498–5504.
9. **Chen, Y., and L. C. Norkin.** 1999. Extracellular Simian Virus 40 transmits a signal that promotes virus enclosure within caveolae. Exp. Cell Res. **246:**83–90.
10. **di Taranto, C., V. Pietropaulo, G. B. Orsi, L. Jin, L. Sinibaldi, and A. M. Degener.** 1997. Detection of BK polyomavirus genotypes in healthy and HIV-positive children. Eur. J. Epidemiol. **13:**653–657.
11. **Dorries, K., and C. Elsner.** 1991. Persistent polyomavirus infection in kidney tissue of patients with disease other then progressive multifocal leucoencephalopathy. Virol. Adv. **10:**51–61.
12. **Drachenberg, C. B., J. C. Papadimitriou, R. Wali, C. Cubitt, and E. Ramos.** 2003. BK polyoma virus allograft nephropathy: ultrastructural features from viral cell entry to lysis. Am. J. Transplant. **3:**1383–1392.
13. **Fishman, J. A.** 2002. BK virus nephropathy—polyomavirus adding insult to injury. N. Engl. J. Med. **347:**527–530.
14. **Fishman, P. H.** 1982. Internalization and degradation of cholera toxin by cultured cells: relationship to toxin action. J. Cell Biol. **93:**860–865.
15. **Gilbert, J. M., and T. L. Benjamin.** 2000. Early steps of polyomavirus entry into cells. J. Virol. **74:**8582–8588.
16. **Gilbert, J. M., I. G. Goldberg, and T. L. Benjamin.** 2003. Cell penetration and trafficking of polyomavirus. J. Virol. **77:**2615–2622.
17. **Harlow, E., and D. Lane.** 1988. Antibodies: a laboratory manual. Cold Spring Harbor Laboratory, Cold Spring Harbor, N.Y.
18. **Howley, P. M. (ed.).** 1980 Viral oncology. Raven Press, New York, N.Y.
19. **Jin, L., J. Park, S. Lee, B. Park, S. J., K. Song, T. Ahn, S. Hwang, B. Ahn, and K. Ahn.** 2002. Hantaan virus enters cells by clathrin-dependent receptor-mediated endocytosis. Virology **294:**60–69.
20. **Kahan, A. V., D. V. Coleman, and L. G. Koss.** 1980. Activation of human polyomavirus infection-detection by cytologic techniques. Am. J. Clin. Pathol. **74:**326–332.
21. **Khalili, K., and G. L. Stoner (ed.).** 2001. Human polyomaviruses. Wiley-Liss, Inc., New York, N.Y.
22. **Knipe, D. M., and P. M. Howley (ed.).** 2001 Fundamental virology, 4th ed. Lippincott Williams & Wilkins, Philadelphia, Pa.
23. **Koss, L. G. (ed.).** 1992. Diagnostic cytology and its histopathologic basis, 4th ed., vol. 2. Lippincott, Philadelphia, Pa.
24. **Le, P., and I. R. Nabi.** 2003. Distinct caveolae-mediated endocytic pathways target the Golgi apparatus and the endoplasmic reticulum. J. Cell Sci. **116:** 1059–1071.
25. **Machleidt, T., W. P. Li, P. Liu, and R. G. W. Anderson.** 2000. Multiple domains in caveolin-1 control its intracellular traffic. J. Cell Biol. **148:**17–28.
26. **Mantyjarvi, R., H. Karjalainen, and M. Laaksonen.** 1984. Cell-mediated immune reaction against BK virus-transformed cells. Cancer Immunol. Immunother. **17:**28–32.
27. **Mantyjarvi, R., O. Meumiam, L. Vihma, and B. Berglund.** 1973. Human papovavirus (B.K.), biological properties and seroepidemiology. Ann. Dis. Res. **5:**283–287.
28. **Marsh, M., and A. Helenius.** 1989. Virus entry into animal cells. Adv. Virus Res. **36:**107–151.
29. **Nabi, I. R., and P. U. Le.** 2003. Caveolae/raft-dependent endocytosis. J. Cell Biol. **161:**673–677.
30. **Narayan, S., R. Barnard, and J. Young.** 2003. Two retroviral entry pathways distinguished by lipid raft association of the viral receptors and differences in viral infectivity. J. Virol. **77:**1977–1983.
31. **Nichols, B. J.** 2002. A distinct class of endosome mediates clathrin-independent endocytosis to the Golgi complex. Nat. Cell Biol. **4:**374–378.
32. **Nichols, B. J., A. K. Kenworthy, R. S. Polishchuk, R. Lodge, T. Roberts, K. Hirschberg, R. D. Phair, and J. Lippincott-Schwartz.** 2001. Rapid recycling of lipid raft markers between the cell surface and Golgi complex. J. Cell Biol. **153:**529–541.
33. **Nickeleit, V., H. H. Hirsch, I. F. Binet, F. Gudat, O. Prince, and P. Dalquen.** 1999. Polyomavirus infection of renal allograft recipients: from latent infection to manifest disease. J. Am. Soc. Nephrol. **10:**1080–1089.
34. **Nickeleit, V., J. Steiger, and M. J. Mihatsch.** 2002. BK virus infection after kidney transplantation. Graft Organ Cell Transplant. **5:**S46–S57.
35. **Nystrom, F. H., E. Chen, L. Cong, Y. Li, and M. Quon.** 1999. Caveolin-1 interacts with the insulin receptor and can differentially modulate insulin signaling in transfected Cos-7 cells and rat adipose cells. Mol. Endocrinol. **13:**2013–2024.
36. **Padgett, B. L., and D. L. Walker.** 1973. Prevalence of antibodies in human sera against JC virus, an isolate from a case of progressive multifocal leukoencephalopathy. J. Infect. Dis. **127:**467–470.
37. **Parton, R. G.** 1994. Ultrastructural localization of gangliosides; GM1 is concentrated in caveolae. J. Histochem. Cytochem. **42:**155–166.
38. **Pelkmans, L., and A. Helenius.** 2002. Endocytosis via caveolae. Traffic **3:**311–320.
39. **Pelkmans, L., and A. Helenius.** 2003. Insider information: what viruses tell us about endocytosis. Curr. Opin. Cell Biol. **15:**414–422.
40. **Pelkmans, L., J. Kartenbeck, and A. Helenius.** 2001. Caveolar endocytosis of simian virus 40 reveals a new two-step vesicular-transport pathway to the ER. Nat. Cell Biol. **3:**473–483.
41. **Pelkmans, L., D. Puntener, and A. Helenius.** 2002. Local actin polymerization and dynamin recruitment in SV40-induced internalization of caveolae. Science **296:**535–539.
42. **Petrogiannis-Haliotis, T., G. Sakoulas, J. Kirby, I. J. Koralnik, A. M. Dvorak, R. Monahan-Earley, U. De Girolami, M. Upton, E. O. Major, L.-A. Pfister, and J. T. Joseph.** 2001. BK-related polyomavirus vasculopathy in a renal-transplant recipient. N. Engl. J. Med. **345:**1250–1255.
43. **Pho, M. T., A. Ashok, and W. J. Atwood.** 2000. JC virus enters human glial cells by clathrin dependent receptor mediated endocytosis. J. Virol. **74:**2288–2292.
44. **Querbes, W., A. Benmerah, D. Tosoni, P. P. Di Fiore, and W. J. Atwood.** 2004. A JC virus-induced signal is required for infection of glial cells by a clathrin- and eps15-dependent pathway. J. Virol. **78:**250–256.
45. **Raptis, L. (ed.).** 2001. SV40 protocols, vol. 165. Humana Press Inc., Totowa, N.J.
46. **Razani, B., A. Schlegel, J. Liu, and M. P. Lisanti.** 2001. Caveolin-1, a putative tumor suppressor gene. Biochem. Soc. Trans. **29:**494–499.
47. **Richterova, Z., D. Liebl, M. Horak, Z. Palkova, J. Stokrova, P. Hozak, J. Korb, and J. Forstova.** 2001. Caveolae are involved in the trafficking of mouse polyomavirus virions and artificial VP1 pseudocapsids toward cell nuclei. J. Virol. **75:**10880–10891.
48. **Roskopf, J., W. Fitzsimmons, N. Ahsan, and D. Laskow.** 2002. The pharmacologic treatment of human polyomavirus infection. Graft Organ Cell Transplant. **5:**S88–S97.
49. **Rothberg, K. G., J. E. Heuser, W. C. Donzell, Y. Ying, J. R. Glenney, and R. G. W. Anderson.** 1992. Caveolin, a protein component of membrane coats. Cell **68:**673–682.
50. **Rothenberger, S., B. J. Iacopetta, and L. C. Kuhn.** 1998. Endocytosis of the transferrin receptor requires the cytoplasmic domain but not its phosphorylation site. Cell **49:**423–431.
51. **Roy, S., R. Luetterforst, A. Harding, A. Apolloni, M. Etheridge, E. Stang, B. Rolls, J. Hancock, and R. G. Parton.** 1999. Dominant-negative caveolin inhibits H-Ras function by disrupting cholesterol-rich plasma membrane domains. Nat. Cell Biol. **1:**98–105.
52. **Schapiro, F., C. Lingwood, W. Furuya, and S. Grinstein.** 1998. pH-dependent retrograde targeting of glycolipids to the Golgi complex. Am. J. Physiol. **27:**C319–C332.
53. **Schlegel, A., V. D. Engelman, J. A. Galbiati, F. Mehta, P. Zhang, X. L. Scherer, and P. E. Lisanti.** 1998. Crowded little caves: structure and function of caveolae. Cell Signal **10:**457–463.
54. **Seganti, L., P. Mastromarino, F. Superti, L. Sinibaldi, and N. Orsi.** 1981. Receptors for BK virus on human erythrocytes. Acta Virol. **25:**177–181.
55. **Shah, K. V.** 1996. Polyomaviruses, p. 2027–2043. *In* B. N. Fields, D. M. Knipe, and P. M. Howley (ed.), Virology. Lippincott-Raven, Philadelphia. Pa.
56. **Shinohara, T., M. Matsuda, S. H. Cheng, J. Marshall, M. Fujita, and K. Nagashima.** 1993. BK virus infection of the human urinary tract. J. Med. Virol. **41:**301–305.
57. **Sieczkarski, S. B., and G. R. Whittaker.** 2002. Influenza virus can enter and infect cells in the absence of clathrin-mediated endocytosis. J. Virol. **76:** 10455–10464.
58. **Singh, R. D., V. Puri, J. T. Valiyaveettil, D. L. Marks, R. Bittman, and R. Pagano.** 2003. Selective caveolin-1-dependent endocytosis of glycosphingolipids. Mol. Biol. Cell **14:**3254–3265.
59. **Sinibaldi, L., P. Goldoni, V. Pietropaulo, C. Longhi, and N. Orsi.** 1990. Involvement of gangliosides in the interaction between BK virus and Vero cells. Arch. Virol. **113:**291–296.
60. **Sinibaldi, L., D. Viti, P. Goldoni, G. Cavallo, C. Caroni, and N. Orsi.** 1987. Inhibition of BK virus haemagglutination by gangliosides. J. Gen. Virol. **68:**879–883.
61. **Smart, E. J., G. A. Graf, A. McNiven, W. C. Sessa, J. A. Engelman, P. E. Scherer, T. Okamoto, and M. P. Lisanti.** 1999. Caveolins, liquid-ordered domains, and signal transduction. Mol. Cell. Biol. **19:**7289–7304.
62. **Sundsfjord, A., T. Flaegstad, R. Flo, A. R. Spein, M. Pedersen, and H. Permin.** 1994. BK and JC viruses in human immunodeficiency virus type 1-infected persons: prevalence, excretion, viremia, and regulatory regions. J. Infect. Dis. **169:**485–490.
63. **Toomre, D., and K. Simons.** 2000. Lipid rafts and signal transduction. Mol. Biol. Cell **1:**31–41.
64. **Tran, D., J. L. Carpentier, F. Sawano, P. Gorden, and L. Orci.** 1987. Ligands internalized through coated and noncoated invaginations follow a common intracellular pathway. Proc. Natl. Acad. Sci. USA **84:**7957–7961.
65. **White, J., K. Matlin, and A. Helenius.** 1981. Cell fusion by Semliki Forest, influenza and vesicular stomatitis viruses. J. Cell Biol. **89:**674–679.